



Contents lists available at ScienceDirect

International Journal of Electronics and Communications (AEÜ)

journal homepage: www.elsevier.com/locate/aeue

Regular Paper

Metamaterial based broadband RF absorber at X-band

Kadir Ozden^{a,*}, Okan Mert Yuicedag^{b,c}, Hasan Kocer^{b,*}^a Defense Sciences Institute, Turkish Military Academy, 06654 Ankara, Turkey^b Department of Electronics Engineering, Turkish Military Academy, 06654 Ankara, Turkey^c TUBITAK Informatics and Information Security Research Center, 41470 Kocaeli, Turkey

ARTICLE INFO

Article history:

Received 14 December 2015

Accepted 2 May 2016

Keywords:

Metamaterial

X-band broadband absorber

Radar absorbing materials

Stealth technology

ABSTRACT

Metamaterial based electromagnetic wave absorbers may provide perfect absorption over significant range of electromagnetic spectrum. With perfect and broadband absorption, metamaterial absorbers play an important role in stealth technology. In this paper, design, simulation and measurements of a novel X-band (8–12 GHz) metamaterial broadband absorber are presented. An absorber operating in the middle of the microwave X-band is obtained by selecting differently sized unit cells and placing their resonant frequencies close to each other. The paper presents two absorbers which consist of different number of unit cells. The first absorber has 12 unit cells (KOH12) while the other has 16 unit cells (KOH16). It is observed that the simulation results are in good agreement with the measurements. Measurement bandwidth for an absorption level of 80% is 2.73 GHz for KOH12 and 2.55 GHz for KOH16. These are the highest absorption levels for planar metamaterial absorbers at X-band. The absorption mechanism of broadband metamaterial absorber is also investigated by using electric and magnetic field distribution. Results of this study are promising for the stealth applications as absorbing elements against X-band radars.

© 2016 Elsevier GmbH. All rights reserved.

1. Introduction

Metamaterials are periodically arranged new type of composites that exhibit exceptional electromagnetic properties not readily observed in nature. One of the features discovered in recent years is performing perfect absorption against the incident electromagnetic wave. Due to their simple design, easy fabrication process, perfect and broadband absorption features as well as tunable and controllable absorption characteristics, metamaterial absorbers can be used in stealth technology toward remote sensing applications over a significant range of electromagnetic spectrum from microwave to optics.

Stealth technology which is a valuable research area for electronic warfare provides passive counter-measurement. It is a combination of technologies to reduce the distances at which a target can be detected. Stealth applications particularly deal with radar cross section reduction (RCS). RCS of relevant targets can be defined as the visibility in radar or the amount of reflected radar signal [1]. Therefore, reduction of RCS is important for military and electronic warfare applications. Current techniques to reduce

radar cross section are mainly based on shaping the surface of target and absorbing the incident electromagnetic wave. Shaping the target is a good technique but not enough in itself for desired purpose because of poor aerodynamic performance, increased costs and more maintenance requirements. Due to these drawbacks of shaping the target, radar absorbing materials are also necessary for stealth technology. For the radar absorbing materials, design, weight, thickness, absorptivity, environmental resistance and mechanical strength are the key factors. Moreover, development of radar absorbing materials with low density and high strength is a challenging task. Compared to the conventional microwave absorbers, metamaterial based absorbers can be an alternative solution of reducing RCS due to the high absorption, low density, thin thickness and unlimited frequency performance over a large range of electromagnetic spectrum.

The first and probably the most known definition of metamaterials is the one composed by metal and dielectric materials exhibiting simultaneously negative real parts of both permittivity (ϵ_r) and permeability (μ_r) [2]. Having simultaneously negative ϵ_r and μ_r , incident wave in the metamaterials has different properties such as backward wave propagation, negative refractive index and phase velocity. With their unique properties, they get considerable interest about lens with perfect focusing [3], cloaking [4], antenna radiation [5] and electromagnetic wave absorption [6] applications. As electromagnetic wave absorbers, they can be used for

* Corresponding authors.

E-mail addresses: kozden@kho.edu.tr, tatarkadir06@gmail.com (K. Ozden), mert.yuicedag@tubitak.gov.tr (O.M. Yuicedag), drhasankocer@gmail.com, hkocer@kho.edu.tr (H. Kocer).

radar cross section reduction [7], decreasing sidelobe radiation in antennas and the reduction of electromagnetic interference [8].

First studies about metamaterials have looked at its negative index of refraction property. Victor G. Veselago was the first scientist who started to work on this property in 1968 [9]. The first experimental verification of negative index of refraction was confirmed by Sir John Pendry et al. [10]. Landy et al. have studied the use of metamaterials as electromagnetic wave absorbers with near perfect absorption in 2008 for the first time [11]. Following on the study of Landy, Wang et al. [6] and Cheng et al. [12] presented polarization insensitive and wide angle metamaterial absorbers. After that, a resonant absorber with three-layer unit cell was presented by Li et al. [13]. Moreover, Lee et al. designed a bandwidth-enhanced microwave absorber where two absorption peaks were not far away from each other, unlike other dual band absorbers [14]. Two well known Electric Field Driven LC (ELC) resonator structure were combined to obtain dual band absorbance [15]. The proposed absorber had two distinct frequency of absorption near to 5.5 GHz and 9.5 GHz with peak absorbance of 99.1% and 99.9%, respectively. By comprising of 2×2 array of absorber [15] oriented in different directions, a triple band polarization insensitive absorption was achieved [16]. On the other hand, Bian et al. [17], Bhattacharyya et al. [18] and Ayop et al. [19] prepared the unit cell of the metamaterial consisting of concentric square and circular rings with three distinct absorption peaks with having several characteristics like wide-angle and polarization-insensitivity. However, each absorption bandwidth was still very narrow due to the resonant behavior of metamaterial elements, limiting the potential application of these absorbers in the fields of cloaking and stealth technology.

Hence, developing broadband metamaterial absorbers has become a challenging task. Genetic algorithms or multilayer structures have been used to enhance the operating frequency of the metamaterial absorber such as designing them in multi-band and broader bandwidth. By combining five unit cell structures with different geometric dimensions into a coplanar unit cell, a broadband absorption with a full width at half maximum (FWHM) bandwidth of 970 MHz was obtained by Lee and Lee [20]. By exploiting the scalability property of metamaterials, Kollatou et al. implemented efficient multi-band and broadband structures [21]. A donut-shape metamaterial absorber with different sizes working in multiple bands was presented by Park et al. [22]. The broad bandwidth metamaterial absorber was achieved by overlapping the absorption peaks of the unit cells when their peaks closed to each other. A planar isotropic broadband metamaterial absorber was proposed by Gu et al. [23]. It consists of hexagonal metal dendritic units having different sizes corresponding to different resonant frequencies. The absorption level greater than 80% of this dendritic isotropic absorber is 2.35 GHz in the X-band. A new design was implemented by using a 2×2 array using two different variants of swastika-like structure [24]. It had 6.5% bandwidth around absorption frequency of 10.38 GHz.

In addition, methods involving the use of lumped elements can also widen the working band for microwave frequencies [25]. However, using lumped elements is not feasible, especially in the THz, IR or optical frequencies. Other way of widening the absorption is the multilayer structure in which resonators share the same ground plane [26]. This stacked metamaterial absorber is also used to induce a successive anti-reflection in wide frequency range. With further advancements in absorbing devices, the parameters of metamaterial absorbers such as large bandwidth, high absorption, reduced thickness, and so on need to be further improved. Moreover, they are complicated and not easy to fabricate. The drawback of this design is that it needs four layers at least, resulting in the increment of overall thickness. Eventually, compared to the conventional millimeter wave absorbers which are physically

thick and their frequency performance is limited, metamaterial absorbers can be used in many applications due to their advantages of simple design, easy fabrication, stable performance as well as extended bandwidth. So, it is important to understand the pros and cons of the metamaterial based electromagnetic wave absorbers. Therefore, the geometrical parameters and thermal effect of metamaterial based absorbers were investigated [27,28].

In this paper, unlike the narrow-band absorbers in the previous studies, a thin broadband metamaterial absorber is proposed. The proposed metamaterial absorber consists of two shaped rectangular metallic rings with a dielectric layer on top of a metallic ground plane. Primarily, a dual band metamaterial absorber is designed and the effect of geometrical parameters on absorption is investigated. A broadband metamaterial absorber has been obtained at X-band by placing neighboring resonant frequencies of differently sized unit cells together in a super cell. Simulations, fabrication, and measurements for the proposed absorbers have been presented in this paper. The broadband metamaterial absorber can be obtained using a single-layer microstrip technology, which has the advantages of simple structure and easy fabrication. In the case of normal incidence, the absorbers which consist of 12 (KOH12) and 16 (KOH16) scaled unit cells yield absorption rates greater than 80% in the frequency range from 8.86 GHz to 11.41 GHz and from 9.09 GHz to 11.08 GHz, respectively. Eventually, the absorption level of these absorbers are compared and the mechanism of the absorption is explained by electric and magnetic field distributions.

2. Design, simulation, fabrication and measurement

The proposed metamaterial absorber consists of two metallic layers separated by a dielectric material. Top layer consists of two concentric square rings. The inner ring is composed of ELC resonator connected by the inductive wire parallel to the splits [11]. The outer ring is also made up of split ring resonator (SRR) with oppositely oriented splits. Bottom layer is metallic continuous ground plane. A schematic diagram of the unit cell can be seen in Fig. 1(a). These metallic layers are selected as copper which has $17 \mu\text{m}$ thickness and its frequency independent conductivity (σ) is $5.8 \times 10^7 \text{ S/m}$. The dielectric material is epoxy glass cloth laminate (FR4) which has 0.75 mm thickness and its relative dielectric permittivity (ϵ_r) is 3.6 and the loss tangent ($\tan \delta$) is 0.03. The simulated metamaterial has the dimensions, in millimeters, of: $L_1 = 6.67$, $L_2 = 5.33$, $L_3 = 3.25$, $w = 0.50$, $g = 0.33$ and $d = 0.54$.

In this study, the design and analysis are carried out with CST Microwave Studio. In the simulation setup, the absorber is illuminated by a polarized plane wave in 7–13 GHz frequency band. The plane wave propagates along $-z$ direction. The polarization of the electric field vector is along the $-y$ -axis. The boundary conditions are perfect electric (PEC) in the yz -plane and perfect magnetic (PMC) in the xz -plane.

For the design of an efficient and reliable metamaterial absorber, it is necessary to minimize both the reflection and transmission of the incident waves, exploiting the complex interactions of the metamaterial with the impinging radiation. Such a requirement stems from the definition of the absorption, obtained in terms of the S -parameters, as $A(f) = 1 - T(f) - R(f)$ where $T(f) = |S_{21}(f)|^2$ is the transmittance and $R(f) = |S_{11}(f)|^2$ is the reflection of the metamaterial absorber. $T(f)$ is zero due to the presence of the continuous copper ground plane. Thus, the total absorption is calculated only by considering the reflection coefficient via relation $A(f) = 1 - R(f)$. In order to achieve the maximum absorption, the reflection should be minimized. The simulation results for the metamaterial perfect absorber are presented in Fig. 1(b). It can be observed that the reflection of the absorber drops to a min-

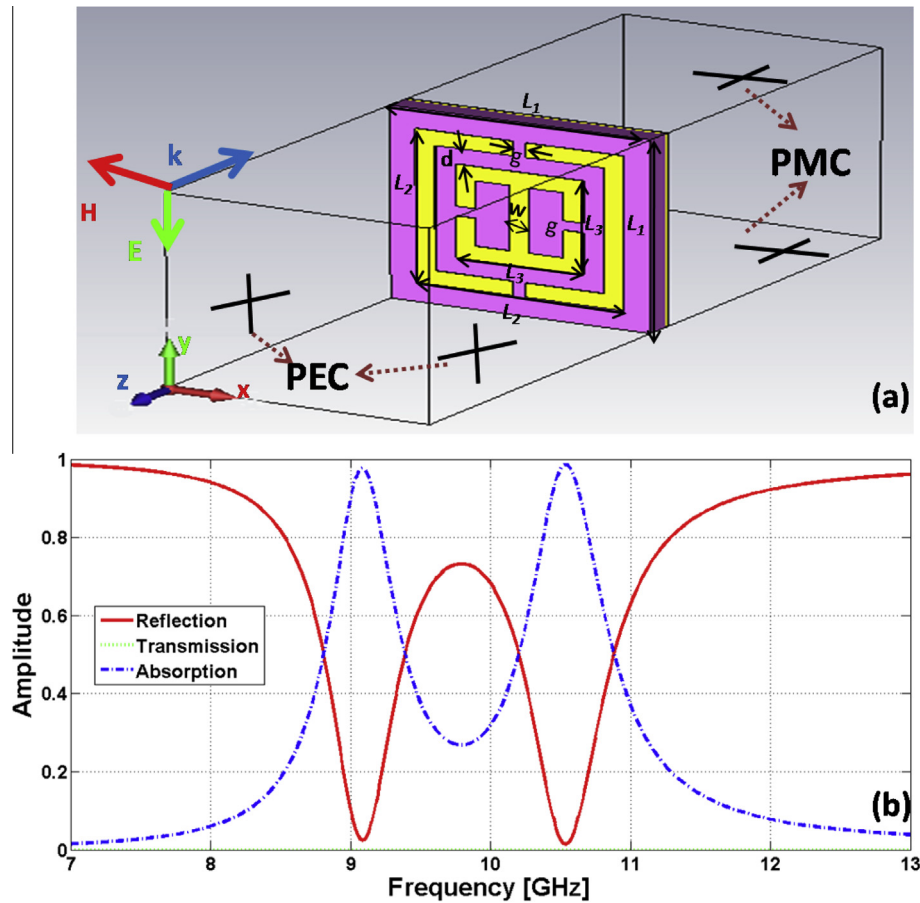


Fig. 1. (a) Perspective view of the simulation. (b) Simulated absorption, transmission and reflection of one unit cell.

imum at both frequency of 9.10 GHz and 10.53 GHz. The corresponding absorption is found out from the equation above as of 97.95% and 98.40%, respectively.

2.1. Parametric analyses of a unit cell

The analyses are carried out by measuring $S_{11}(f)$ and $S_{21}(f)$ under normal incidence in the simulation. Due to the shielding of the bottom metal plate ($T(f) = 0$), $A(f) = 1 - R(f)$. It can be understood from the equation that the absorption and reflection curves follow opposite trends. By means of changing geometric configuration of a unit cell, it is enough to investigate absorption response of the absorber at resonant frequencies. The first simulation is performed for different values of g while the other parameters are kept fixed as $L_1 = 6.67$ mm, $L_2 = 5.33$ mm, $L_3 = 3.25$ mm, $w = 0.50$ mm and $d = 0.54$ mm. Results are presented in Fig. 2. Decreasing the capacitance of the system will increase the resonant frequency (f_0) [29]. Due to the fact that $f_0 \approx 1/\sqrt{LC}$, an enlargement of the split width from $g = 0.17$ mm to $g = 1.33$ mm increases f_0 .

The second simulation is performed by changing d while the other parameters are kept fixed as $L_1 = 6.67$ mm, $L_2 = 5.33$ mm, $w = 0.50$ mm and $g = 0.33$ mm. Since the outer ring is fixed, increasing the gap distance will also decrease the size of the inner ring. Increasing the gap size between the rings decreases both mutual capacitance and inductance and increases f_0 [29]. Results are seen in Fig. 3.

The last simulation is performed by changing w for different values while the other parameters are kept fixed as $L_1 = 6.67$, $L_2 = 5.33$, $L_3 = 3.25$, $g = 0.33$ and $d = 0.54$. Increasing the metal

width increases the inductance and capacitance. Changing w primarily effects f_0 as shown in Fig. 4. These inductance and capacitance effects on the absorption frequency can be used for optimizing the resonance frequencies to achieve broadband bandwidth [30].

2.2. Design of a super unit cell

The super unit cell is implemented to create efficient broadband structures by exploiting the scalability property of metamaterials. Explicitly, by multiplying the dimensions of the original unit cell along the x - and y -axis by a scaling factor s_i , the center absorption frequency can be downshifted ($s_i > 1$) or upshifted ($s_i < 1$), whereas the absorption curve retains its initial shape and fractional bandwidth. No scaling is applied along the z -direction.

An absorber operating in the middle of the microwave X-band is obtained by selecting differently sized unit cells and placing resonant frequencies close to each other. Considering the coupling effects of unit cells, the location of the unit cell is also optimized in the super cell to improve the absorption bandwidth of metamaterial absorber. Each unit cell is scaled by a factor s_i , where $i = 1:16$ as shown in Fig. 5. When s_i decreases, the resonant frequencies shift upper frequencies.

Two super cells which consist of 12 and 16 scaled unit cells are simulated. Fig. 6 shows the simulated absorption characteristics of KOH12 and KOH16 with different arrangement and array directions. The differences of scaling factors between the proposed metamaterial absorbers have caused different bandwidths and absorption levels. This is mainly due to the combination of different geometric dimensions of unit cells shifting the resonance

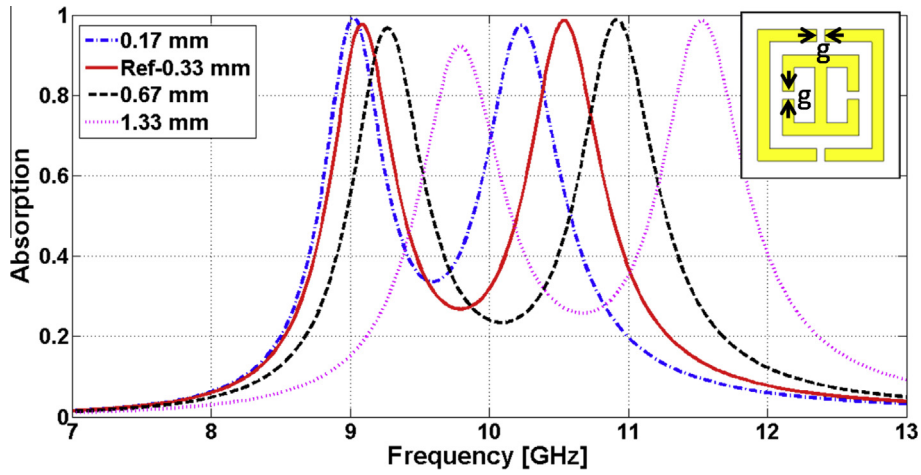


Fig. 2. Absorption versus frequency for different values g .

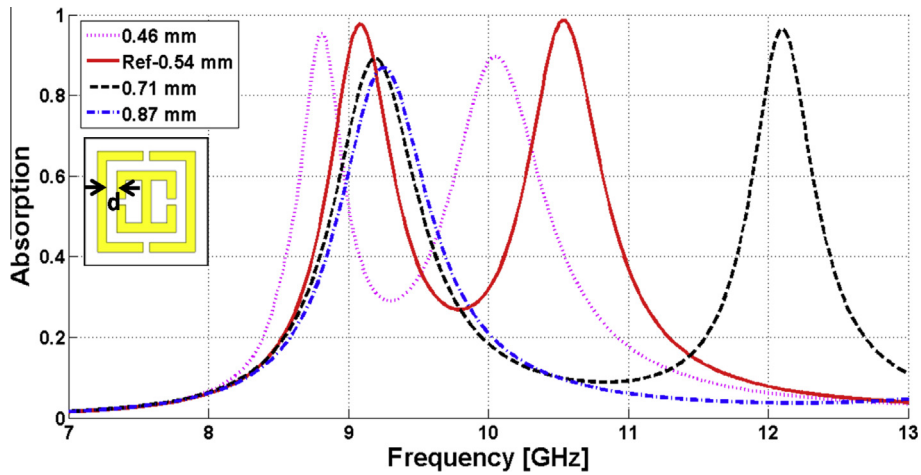


Fig. 3. Absorption versus frequency for different d .

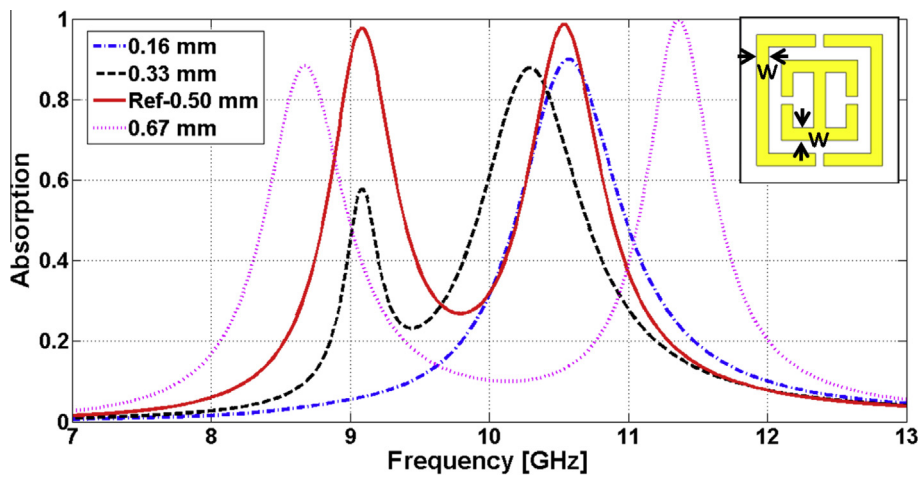


Fig. 4. Absorption versus frequency for different w .

frequency to lower or higher values. It is observed that KOH12 and KOH16 have similar absorption bandwidths in X-band. However, by selecting scale factors close to each other and increasing the number of unit cells, it is possible to get smoother absorption level around 90%. This improved absorption bandwidth of KOH16 is

mainly due to the electromagnetic field coupling between the neighbor unit cells. The bandwidth can be improved with using different absorber designs which have more than two resonance frequencies. However, the resonance frequencies must satisfy the condition that they should be close to each other.

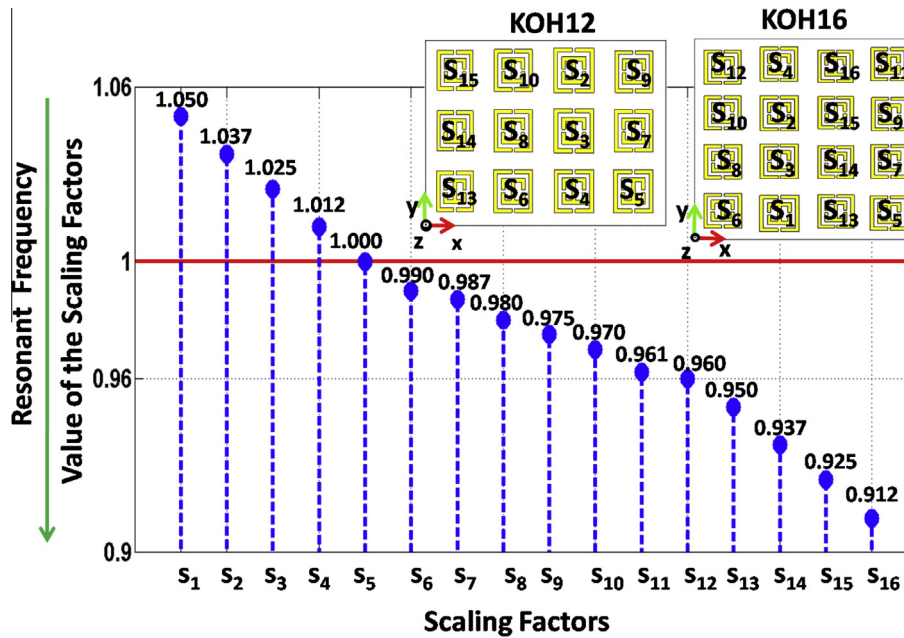


Fig. 5. Scaling factors of KOH12 and KOH16.

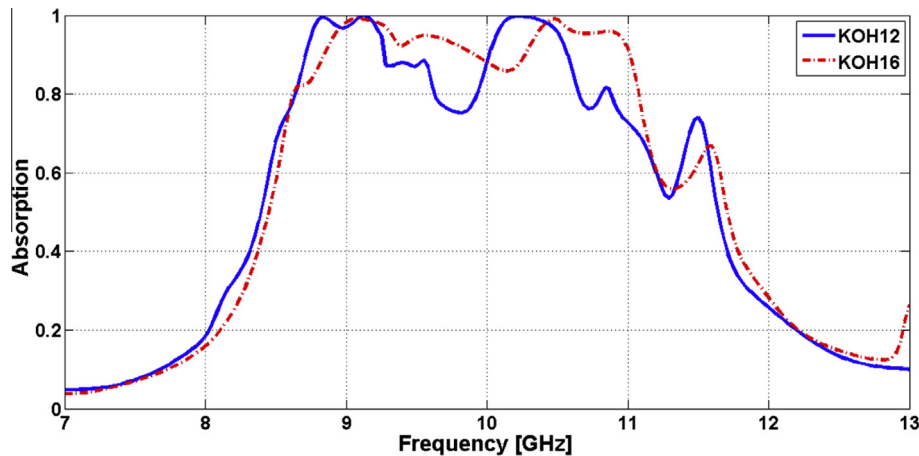


Fig. 6. Absorption spectrum of KOH12 and KOH16.

The simulated absorption of the metamaterial absorber is also investigated for different incident angles (θ) while maintaining the direction of electric field vector along the $-y$ -axis, as shown in Fig. 7(a and b). With regard to oblique incidences, the simulated responses for both KOH12 and KOH16 show that the absorption remains high for incident angles up to 40° . When the incidence angle is 60° , the absorption curve does not maintain the integrity of bandwidth. Overall, the proposed absorber ensures a reasonable absorption performance against oblique incident electromagnetic waves for a range of angle. KOH16 has better absorption performance depending on the angle than KOH12. The proposed absorbers have polarization dependent characteristics due to non-symmetrical structure of metallic units of the first layer.

2.3. Fabrication and measurement of the metamaterial absorber

To verify the simulation results, two planar $9.6 \text{ cm} \times 9.6 \text{ cm}$ (KOH12) and $12.5 \text{ cm} \times 12.5 \text{ cm}$ (KOH16) supercell prototypes have been fabricated through printed circuit board (PCB)

technique on a FR4 substrate as seen in Fig. 8(a and b). The absorber has a thickness of $\lambda/18$ where λ is the operating wavelength corresponding to the middle of the absorption bandwidth. In the experimental setup, as shown in Fig. 8(c), a vector network analyzer (Net Rohde & Schwarz ZVL, 9 KHz – 13.6 GHz) and a pair of double-ridged waveguide horn antennas (HF907 800 MHz – 18 GHz) are used. The distance between the horn antennas is set to 45 cm in order to prevent the near field effects on the reflection and the metamaterial absorber is located 90 cm away from the antennas. Many absorbers are placed around the metamaterial absorber sample and between the horn antennas to eliminate the electromagnetic interference from the surrounding environment and antennas. The horn antennas serving as the transmitter and receiver are connected to the network analyzer by using low loss flexible cables in order to measure the reflection coefficient. The back plane of the metamaterial absorber which is completely metallic is measured as the first phase. In the second phase, the reflection coefficient is measured by using top layer of the metamaterial absorber.

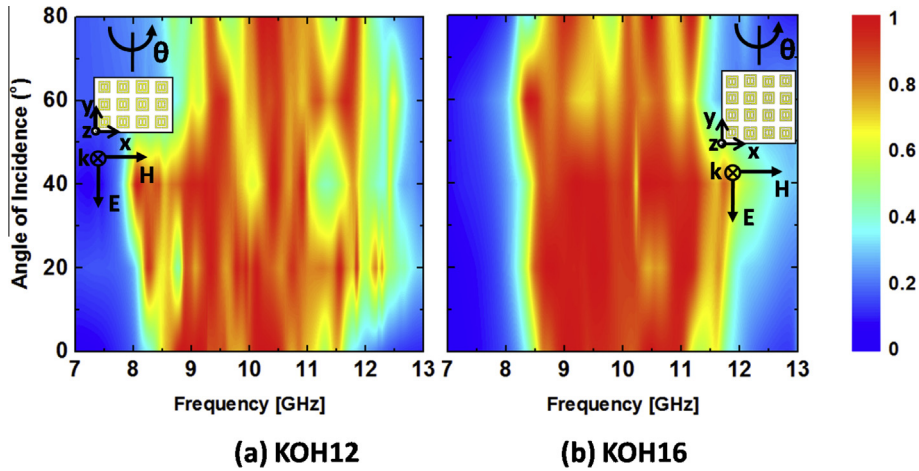


Fig. 7. Simulated absorption at different incident angles for (a) KOH12 and (b) KOH16 (θ corresponds to the angle of incidence).

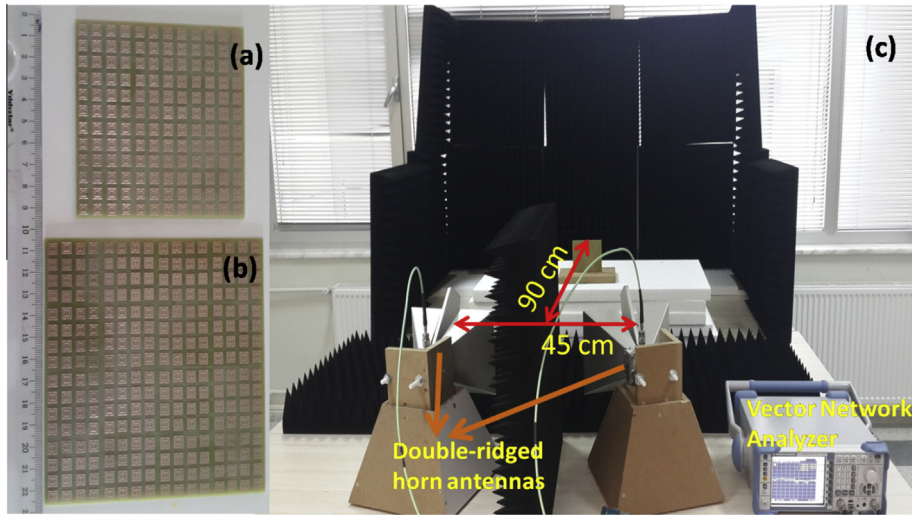


Fig. 8. (a) Photograph of the fabricated KOH12. (b) Photograph of the fabricated KOH16. (c) The experimental setup.

3. Results and discussions

The frequency characteristic of the absorptions are presented in Fig. 9(a and b). KOH12 operates in the X-band and yields absorption rates greater than 80% in the frequency range from 8.71 GHz to 11.44 GHz. KOH16 operates in the X-band as well and yields absorption rates greater than 80% and 90% in the frequency range from 8.86 GHz to 11.41 GHz and from 9.09 GHz to 11.08 GHz, respectively. The measured absorption bandwidths are 2.73 GHz for KOH12 and 2.55 for KOH16 at 80% absorption level. KOH12 has greater bandwidth than KOH16. However, the absorption above 90% level of KOH16 is more closer to perfect absorption in the simulation and measurement results. The measurement results show that increasing the number of unit cell in super cell does not change frequency bandwidth. On the other hand, this increment improves the absorption level.

Despite increasing the number of unit cells in a super cell, bandwidth of the absorber does not increase due to super cell size which is electrically comparable with working wavelength. Overall, RF simulation results are in a reasonable agreement with the measurements. This reasonable and anticipated difference can be primarily attributed to fabrication tolerances and the fluctuation of the substrate's electric characteristics around their nominal

values. Moreover, the illustrated plane wave with ridged waveguide horn antennas is not same as the simulation setup.

To better understand the physical mechanism of the broadband metamaterial absorber, the electric and magnetic field distributions are simulated at 9.18, 9.76 and 10.52 GHz resonance frequencies of KOH16 and the surface current distribution is simulated on top and bottom of the proposed absorber at 9.18 GHz. The nature of this absorption can be understood from Fig. 10. At different resonant frequencies, the electric field distribution is concentrated strongly in the vicinity of the open gaps, while the magnetic field distribution is concentrated strongly in the vicinity of the inductive ring parallel to the split-wire. The magnetic field distribution is strongly coupled to the specific unit cell at 9.18 and 10.52 GHz. Therefore, the absorption of these frequencies are very close to the perfect absorption level.

It is observed that the direction of current densities of the bottom and top surfaces are opposite and individual square loops are occurred on the top of structure, as shown in Fig. 11. Therefore, the magnetic resonator response is resourced from the opposite directions of those currents [18]. Meanwhile, absorptions at the distinct frequencies are caused by these square current loops owing to a dipolar response which contributes to ϵ_r at 9.18 GHz. The electric resonance response is observed at top of the shaped metallic layer.

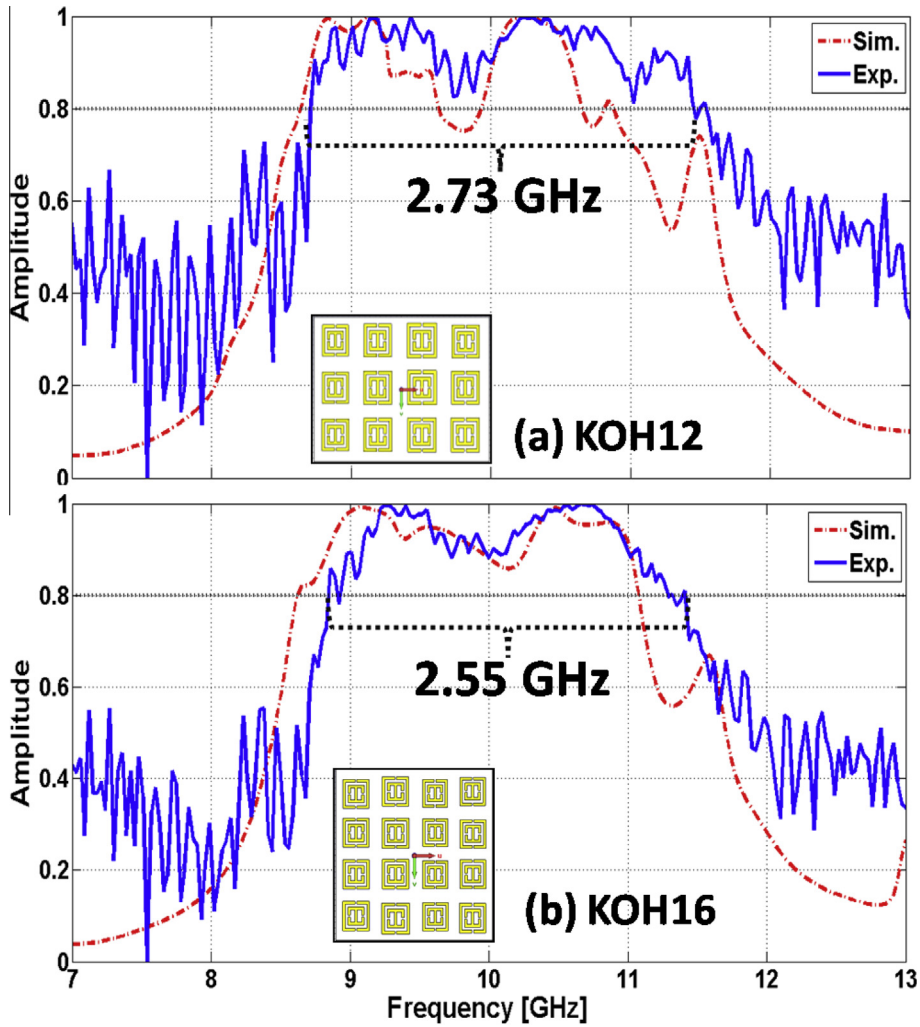


Fig. 9. (a) Absorption spectrum of KOH12. (b) Absorption spectrum of KOH16.

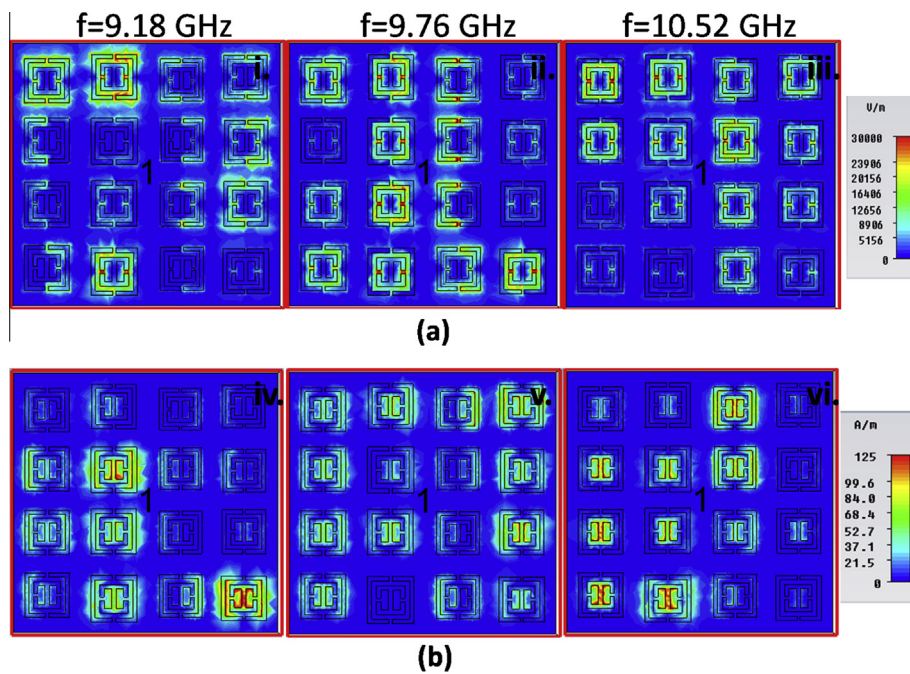


Fig. 10. (a) Electric field distribution of the metamaterial absorber, $|E|$ field. (b) Magnetic field distribution of the metamaterial absorber, $|H|$ field.

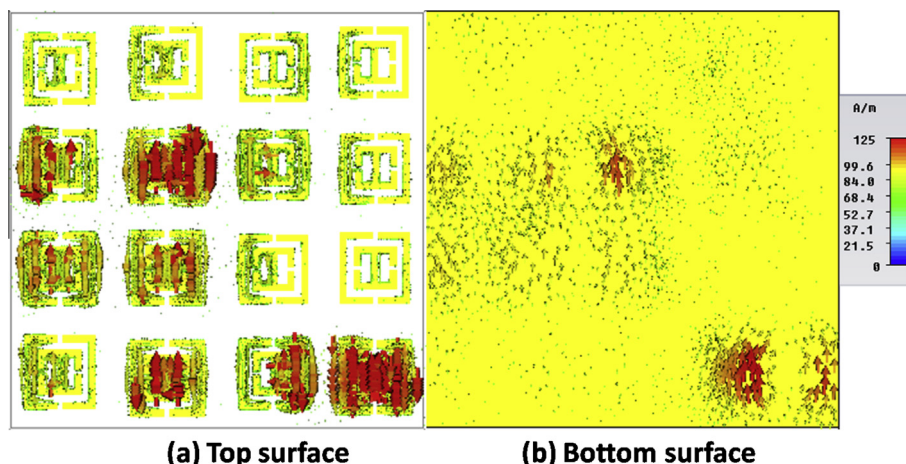


Fig. 11. (a) Surface current distribution on (a) top surface and (b) bottom surface at 9.18 GHz of the metamaterial absorber.

Due to the circulating displacement current between the two metallic layers, magnetic resonance response are also occurred. Therefore, the working principle of the proposed metamaterial absorber is absorption of the incident electric fields by using metallic electric resonators and absorption of incident magnetic fields by exciting magnetic resonances derived from anti-parallel currents.

4. Conclusion

In this paper, the X-band metamaterial based absorbers with broad bandwidth are designed, fabricated and measured. The broadband absorption is achieved by getting resonant frequencies of unit cells close to each other. By decreasing scaling factors of unit cell, the center frequency shifts to upward frequencies. It is observed that increasing the number of unit cells caused smoother absorption level. Although KOH12 has greater absorption bandwidth than KOH16, the simulated and measured absorption level of KOH16 gets close to the perfect absorption. The results show that the simulation results are in good agreement with the measurements. The absorption performance of the KOH12 and KOH16 is also maintained for oblique incidences less than 40° . This kind of absorber finds its use in many practical applications such as stealthy technology as electromagnetic wave absorbing materials to reduce radar cross section.

Acknowledgements

Authors would like to thank Dr. E.U. Aydin, Dr. A.E. Yilmaz and Miss S. Can for their contributions in preparing the experimental setup and 3rd AFSMC for their cooperation to fabricate the samples. Note that, K. Ozden is supported by The Scientific and Technological Research Council of Turkey (TUBITAK) through a postgraduate scholarship program.

References

- [1] Knott E, Shaeffer J, Tuley M. Radar cross section. 2nd ed. Boston: Artech House; 1993.
- [2] Bilotti F, Sevgi L. Metamaterials: definitions, properties, applications, and FDTD-based modeling and simulation (Invited Paper). Int J RF Microw Comput Aided Eng 2012;22(4):422–38.
- [3] Pendry JB. Negative refraction makes a perfect lens. Phys Rev Lett 2000;85(18):3966–9.
- [4] Schurig D, Mock JJ, Justice BJ, Cummer SA, Pendry JB, Starr AF, et al. Metamaterial electromagnetic cloak at microwave frequencies. Science 2006;314(5801):977–80.
- [5] Si LM, Lv X. CPW-FED multi-band omni-directional planar microstrip antenna using composite metamaterial resonators for wireless communications. Prog Electromagn Res 2008;83:133–46.
- [6] Wang B, Koschny T, Soukoulis CM. Wide-angle and polarization-independent chiral metamaterial absorber. Phys Rev B 2009;80(3):0331081–83.
- [7] Munk BA. Frequency selective surfaces. New York: John Wiley & Sons; 2000.
- [8] Emerson WH. Electromagnetic wave absorbers and anechoic chambers through the years. IEEE Trans Antennas Propag 1973;21(4):484–90.
- [9] Veselago VG. The electrodynamics of substances with simultaneously negative values of ϵ and μ . Sov Phys Usp 1968;10(4):509–14.
- [10] Pendry JB, Holden AJ, Robbins DJ, Stewart WJ. Magnetism from conductors and enhanced nonlinear phenomena. IEEE Trans Microw Theory Technol 1999;47(11):2075–84.
- [11] Landy NI, Sajuyigbe S, Mock JJ, Smith DR, Padilla WJ. Perfect metamaterial absorber. Phys Rev Lett 2008;100(20):2074021–24.
- [12] Cheng Y, Yang H, Cheng Z, Wu N. Perfect metamaterial absorber based on a split-ring-cross resonator. Appl Phys A 2011;102(1):99–103.
- [13] Li MH, Yang HL, Hou XW. Perfect metamaterial absorber with dual bands. Prog Electromagn Res 2010;108:37–49.
- [14] Lee J, Lim S. Bandwidth-enhanced and polarisation-insensitive metamaterial absorber using double resonance. Electron Lett 2011;47(1):8–9.
- [15] Bhattacharyya S, Srivastava KV. An ultra thin electric field driven LC resonator structure as metamaterial absorber for dual band applications. Electromagnetic theory (EMTS), proceedings of 2013 URSI international symposium on IEEE. p. 722–5.
- [16] Bhattacharyya S, Srivastava KV. Triple band polarization-independent ultrathin metamaterial absorber using electric field-driven LC resonator. J Appl Phys 2014;115(6):064508.
- [17] Bian B, Liu L, Wang S, Kong X, Zhang H, Ma B. Novel triple-band polarization-insensitive wide-angle ultra-thin microwave metamaterial absorber. J Appl Phys 2013;114(19):194511.
- [18] Bhattacharyya S, Ghosh S, Srivastava KV. Triple band polarization-independent metamaterial absorber with bandwidth enhancement at X-band. J Appl Phys 2013;114(9):094514.
- [19] Ayop O, Rahim MKA, Murad NA, Samsuri NA, Dewan R. Triple band circular ring-shaped metamaterial absorber for X-band applications. Prog Electromagn Res 2014;39:65–75.
- [20] Lee HM, Lee HS. A method for extending the bandwidth of metamaterial absorber. Int J Antennas Propag 2012.
- [21] Kollatou TM, Dimitriadis AI, Assimonis SD, Kantartzis NV, Antonopoulos CS. A family of ultra-thin, polarization-insensitive, multi-band, highly absorbing metamaterial structures. Prog Electromagn Res 2013;136:579–94.
- [22] Park JW, Van Tuong P, Rhee JY, Kim KW, Jang WH, Choi EH, et al. Multi-band metamaterial absorber based on the arrangement of donut-type resonators. Opt Exp 2013;21(8):9691–702.
- [23] Gu S, Su B, Zhao X. Planar isotropic broadband metamaterial absorber. J Appl Phys 2013;114(16):163702.
- [24] Ghosh S, Bhattacharyya S, Srivastava KV. Bandwidth-enhancement of an ultrathin polarization insensitive metamaterial absorber. Microw Opt Technol Lett 2014;56(2):350–5.
- [25] Cheng YZ, Wang Y, Nie Y, Gong RZ, Xiong X, Wang X. Design, fabrication and measurement of a broadband polarization-insensitive metamaterial absorber based on lumped elements. J Appl Phys 2012;111(4):044902.
- [26] Soheilifarand MR, Sadeghzadeh RA. Design, fabrication and characterization of stacked layers planar broadband metamaterial absorber at microwave frequency. AEU Int Electron Commun 2015;69(1):126–32.
- [27] Ozden K, Yucedag OM, Kocer H. Geometrical parameter investigation of metamaterial absorber for space based remote sensing applications. 7th recent adv in space tech sym (RAST). p. 229–32.

- [28] Ozden K, Yucedag OM, Ozer A, Bayrak H, Isik H, Kocer H. Thermal imaging of RF induced heat loss in a microwave metamaterial absorber. 36th prog electromag res sym (PIERS). p. 793–6.
- [29] Bhattacharyya S, Baradiya H, Srivastava KV. An ultra thin metamaterial absorber using electric field driven LC resonator with meander lines. Antennas and propagation society international symposium (APSURSI) IEEE. p. 1–2.
- [30] Ghosh S, Srivastava KV. An equivalent circuit model of FSS-based metamaterial absorber using coupled line theory. Antennas and wireless propagation letters, IEEE, 14. p. 511–4.